

# The year 2020 in the *European Heart Journal—Cardiovascular Imaging*: part II

**Bernard Cosyns** <sup>1\*</sup>, **Leyla Elif Sade**<sup>2,3</sup>, **Bernhard L. Gerber** <sup>4</sup>,  
**Alessia Gimelli** <sup>5</sup>, **Denisa Muraru**<sup>6,7</sup>, **Gerald Maurer**<sup>8</sup>, and  
**Thor Edvardsen** <sup>9,10</sup>

<sup>1</sup>Department of Cardiology, CHVZ (Centrum voor Hart en Vaatziekten), ICMI (In Vivo Cellular and Molecular Imaging) Laboratory, Universitair Ziekenhuis Brussel, 101 Laarbeeklaan, 1090 Brussels, Belgium; <sup>2</sup>University of Pittsburgh Medical Center, Heart and Vascular Institute, University of Pittsburgh, 4200 Fifth Ave, Pittsburgh, PA 15260, USA; <sup>3</sup>Department of Cardiology, University of Baskent, Bağlica Kampüsü, Dumlupınar Blv. 20. Km, 06810 Etimesgut/Ankara, Turkey; <sup>4</sup>Division of Cardiology, Department of Cardiovascular Diseases, Cliniques Universitaires St. Luc, Pôle de Recherche Cardiovasculaire (CARD), Institut de Recherche Expérimentale et Clinique (IREC), Université Catholique de Louvain, Av Hippocrate 10/2806, Brussels, Belgium; <sup>5</sup>Fondazione Toscana G. Monasterio, Via Giuseppe Moruzzi, 1, 56124 Pisa Pl, Italy; <sup>6</sup>Department of Cardiac, Neurological and Metabolic Sciences, Istituto Auxologico Italiano, IRCCS, Piazzale Brescia 20, 20149 Milan, Italy; <sup>7</sup>Department of Medicine and Surgery, University of Milano-Bicocca, Via Cadore 48, 20900 Monza, Italy; <sup>8</sup>Division of Cardiology, Department of Internal Medicine II, Medical University of Vienna, Spitalgasse 23, 1090 Wien, Austria; <sup>9</sup>ProCardio Center for Innovation, Department of Cardiology, Oslo University Hospital, Rikshospitalet, Oslo Norway and Institute for clinical medicine, University of Oslo, Sognsvannsveien 9, 0372 Oslo, Norway; and <sup>10</sup>KG Jebsen Cardiac Research Centre, Institute for clinical medicine, University of Oslo, Sognsvannsveien 20, NO-0424 Oslo, Norway

Received 11 October 2021; editorial decision 11 October 2021

The *European Heart Journal—Cardiovascular Imaging* was launched in 2012 and has during these years become one of the leading multimodality cardiovascular imaging journal. The journal is now established as one of the top cardiovascular journals and is the most important cardiovascular imaging journal in Europe. The most important studies published in our Journal from 2020 will be highlighted in two reports. Part II will focus on valvular heart disease, heart failure, cardiomyopathies, and congenital heart disease. While Part I of the review has focused on studies about myocardial function and risk prediction, myocardial ischaemia, and emerging techniques in cardiovascular imaging.

## Keywords

review • multimodality imaging • echocardiography • cardiac magnetic resonance • cardiac computed tomography • nuclear cardiology

*European Heart Journal—Cardiovascular Imaging* has successfully consolidated as a multimodality journal during its first 9 years. It has now an important role as a significant resource for cardiologists, specialists in all imaging modalities, and other physicians working in the field of cardiovascular imaging. *European Heart Journal—Cardiovascular Imaging* has successfully consolidated as a multimodality journal and is currently rated as number 20 out of 141 cardiovascular journals in the World with an impressive impact factor of 6.875. The tradition of highlighting the most important studies that were published in the last year is continued.<sup>1,2</sup> In two articles, we will summarize the most important papers from the journal in 2020. Part I has just been published. Part II will focus on cardiomyopathies, congenital heart diseases, valvular heart diseases, and heart failure (HF).

## Position papers and expert consensus documents from the European Association of Cardiovascular Imaging

One important assignment of *European Heart Journal—Cardiovascular Imaging* is to publish position papers, and expert consensus papers from the European Association of Cardiovascular Imaging (EACVI). The journal published recommendations and expert consensus papers in the field of cardiac imaging and also the best research presented at our conferences in 2020. These papers are commented on in more detail elsewhere in the two documents. The journal published important position and expert consensus papers in the field of

\* Corresponding author. Tel +322 476 38 95. E-mail: [bcosyns@gmail.com](mailto:bcosyns@gmail.com)

Published on behalf of the European Society of Cardiology. All rights reserved. © The Author(s) 2021. For permissions, please email: [journals.permissions@oup.com](mailto:journals.permissions@oup.com).

cardiac imaging.<sup>3-6</sup> These papers are commented on in more detail elsewhere in the two documents. The EACVI recommendations on precautions, indications, prioritization, and protection for patients and healthcare personnel during the ongoing pandemic was published together with advises on the role of cardiovascular imaging for myocardial injury in hospitalized COVID-19, and how to use lung ultrasound.<sup>7-9</sup>

The EACVI scientific initiatives committee published four interesting surveys in 2020, including one on global evaluation of echocardiography in patients with COVID-19.<sup>10-13</sup> A new section on how to do different imaging measures and the first ones were on left atrial (LA) and right ventricular (RV) strain.<sup>14,15</sup> The best research presented at our conferences in 2019 was also published.<sup>16-18</sup>

## Cardiomyopathies

Several studies focused on the role of echocardiography to permit an early diagnosis of cardiomyopathy either in probands or family relatives.

Baudry *et al.* sought to evaluate the role of regional left ventricular (LV) strain by two-dimensional (2D) echocardiography in sarcomeric hypertrophic cardiomyopathy (HCM) mutation carriers before the hypertrophic stage. They studied 79 adults [derivation cohort: 38 confirmed HCM patients with LV hypertrophy (LVH+/Gen+), 20 mutation carriers without LVH (LVH-/Gen+), and 21 healthy controls], and explored the accuracy of segmental strain values in a separate validation cohort ( $n=61$ ). They reported that only regional longitudinal strain (LS), but not global strain, was significantly reduced at the early stage of HCM before LVH. The suggested cut-offs were <16.5% for basal anteroseptal segment and <0.76 for the ratio between basal inferoseptal and basal anterolateral segment.<sup>19</sup>

Jurlander *et al.* explored the diagnostic yield of family screening in a retrospective analysis of 286 consecutive family relatives of patients affected by arrhythmogenic cardiomyopathy (AC). They diagnosed 7% with definite and 27% with borderline AC according to the 2010 Task Force criteria. Imaging criteria were less sensitive than electrical abnormalities detected with 12-lead electrocardiogram (ECG), signal-averaged ECG, and Holter monitoring. Only six (2.1%) relatives fulfilled a cardiac magnetic resonance (cMR) diagnostic criterion and one relative fulfilled an echocardiographic criterion.<sup>20</sup>

Early diagnosis of cardiac involvement is a key aspect in AL amyloidosis to improve patient prognosis. Nicol *et al.* proposed a diagnostic score including (i) global LS (GLS)  $\geq -17\%$  (1 point); (ii) apical/(basal + median) LS  $\geq 0.90$  (1 point), and (iii) troponin T  $>35$  ng/L (1 point). In a derivation cohort of 114 patients, a score  $>1$  was associated with sensitivity of 94% and specificity of 97%, with an area under the curve (AUC) of 0.98. They also tested this score on a separate validation cohort of 73 AL amyloid patients and the area under the receiver operating characteristic curve was 0.97 (95% CI 0.90–0.99), suggesting a very high accuracy for diagnosing cardiac involvement in AL amyloid patients. Notably, compared to 76% of patients classified as having cardiac involvement using consensus criteria, this simple score enabled them to classify correctly 90% of patients.<sup>21</sup>

Brand *et al.* used LA strain parameters and regional LV strain alterations (LV relative apical sparing) to evaluate 54 patients with cardiac

amyloidosis and other diseases leading to increased LV wall thickness. They found that LA reservoir strain had a higher diagnostic accuracy than LV relative apical sparing (AUC 0.91 vs. 0.74, respectively). These results indicate that the integration of LA strain analysis into the routine echocardiographic assessment might help to rule in the possible diagnosis of cardiac amyloidosis in patients with unexplained LV 'hypertrophy'.<sup>22</sup>

Clemmensen *et al.* evaluated the prognostic implications of LV myocardial work indices in cardiac amyloidosis. They studied 100 cardiac amyloidosis patients for MACE and all-cause mortality at median follow-up of 490 days. They reported that LV myocardial work evaluated non-invasively by pressure-strain analysis may be of clinical value, as both LV myocardial work index (LVMWI) and apical-to-basal segmental work ratio predicted MACE and all-cause mortality. Combination of LVMWI with the apical-to-basal segmental work ratio allowed to obtain a strong model to predict MACE and mortality in cardiac amyloidosis patients.<sup>23</sup>

In sarcoidosis patients, detection of cardiac involvement at an early stage allows the introduction of anti-inflammatory or cardiac device therapy that can reduce the risk of cardiac dysfunction and sudden death. Kusunose *et al.* evaluated the ventricular function in 139 patients with confirmed sarcoidosis and 52 age- and gender-matched control subjects using speckle-tracking echocardiography (STE). They found that impairment in both basal LV and RV free wall LS (FWLS) was associated with worse outcome, including cardiac death or development of cardiac involvement.<sup>24</sup>

Jurcuț *et al.*<sup>25</sup> collected the latest evidence on multimodality imaging of patients with suspected or confirmed cardiac amyloidosis and provided an excellent review of the role of various techniques presented in an effective and practical manner.

In ischaemic cardiomyopathy, the extent of LV scar burden is known to hold prognostic implications. Abou *et al.* evaluated the association between LV mechanical dispersion (MD) and scar burden by late gadolinium enhancement cMR (LGE cMR) in a retrospective analysis of 96 patients after ST elevation myocardial infarction (STEMI). They showed that LV MD is associated with scar burden infarct core, and border zone in STEMI patients. A prolonged LV MD  $>53.5$  ms was correlated with higher event rates and provided the highest predictive value for the combined endpoint (all-cause mortality and appropriate implantable cardioverter-defibrillator therapy) when compared with other echocardiographic and LGE cMR-derived parameters.<sup>26</sup>

LV fibrosis is a major factor in HCM prognostication, being associated with higher risk of sudden cardiac death and progression to burn-out HCM form. Pagourelis *et al.* reported for the first time a comparison of the diagnostic utility of 2D vs. three-dimensional (3D) LV deformation parameters to predict the fibrosis burden at LGE cMR in 40 patients with HCM and 15 patients with LVH due to hypertension. There was only a modest correlation between 2D and 3D strain parameters, and 2D peak segmental LS was the best strain parameter for tissue characterization and fibrosis detection in HCM patients.<sup>27</sup>

In dilated cardiomyopathy, Hooks *et al.* evaluated the characteristics, predictors, and clinical outcomes of a large cohort of patients with LV thrombus detected on LGE cMR. They compared 48 patients with DCM and LV thrombus with 124 patients with ischaemic cardiomyopathy and 144 patients with DCM without thrombus. They

identified as LV ejection fraction (EF) LGE presence and extent as independent predictors of thrombus in DCM. Compared with patients with LV thrombus in ICM, those with LV thrombus in non ischemic cardiomyopathy (NICM) had a 10-fold higher prevalence of thrombi in other cardiac chambers. The 12-month incidence of embolism associated with LV thrombus was not different between NICM and ICM but both were higher compared with no LV thrombus in NICM. Finally, the performance of echocardiography for the detection of LV thrombus was not different between NICM and ICM.<sup>28</sup> Also in DCM, Xu *et al.* (PMID: 32658979) proposed a remodelling index defined as the cubic root of the LV end-diastolic volume divided by the mean LV wall thickness on basal short-axis slice to reflect LV wall stress according to Laplace's law and evaluated the prognostic value in 412 patients. Cox regression showed that this remodelling index, LGE presence, and log (N-terminal pro-B-type natriuretic peptide) were independent predictors of the primary endpoint of overall mortality and heart transplantation while the index and extracellular volume were independent predictors of the secondary endpoint adding HF hospitalization. The addition of remodelling index (RI) to LVEF and LGE presence showed significantly improved global prediction of primary and secondary endpoints. Furthermore, RI derived from echocardiography also showed independent prognostic value for primary and secondary endpoints with clinical risk factors.<sup>29</sup> Another study by Putko *et al.* pointed to the important role of LA remodelling by cMR in HF. In 86 patients with Class C HF in the Alberta Heart Failure Etiology and Analysis Research (HEART) project, LA volume was negatively correlated with LVEF and positively correlated with LV mass in HF and reduced EF (HF<sub>r</sub>EF) but not in HF<sub>p</sub>EF. LA volume at end-diastole was associated with the composite endpoint in HF<sub>r</sub>EF but not HF<sub>p</sub>EF. This supports the hypothesis that the pathophysiologic underpinnings of HF<sub>p</sub>EF and HF<sub>r</sub>EF are different, and atrial remodelling encompasses distinct components for each HF subtype.<sup>30</sup>

In apical hypertrophic cardiomyopathy, Yang *et al.* used cMR to evaluate 1332 consecutive patients for LV apical aneurysms. They found such aneurysm in 2.3% of their population. Compared with apical hypertrophy patients without LV aneurysm, the proportion of systolic mid-cavity obstruction and LGE presence, and the LGE extent in apical HCM (ApHCM) patients with LVAA were significantly higher. Kaplan–Meier curves showed that the event-free survival rate in ApHCM patients with LVAA was significantly lower than that in apical hypertrophy patients without LV aneurysms. This suggests that although rare, this condition, which is often missed by echocardiography can be reliably detected with cMR and is associated with a higher risk of adverse cardiovascular events compared with apical hypertrophy without LV apical aneurysm.<sup>31</sup> Augusto *et al.* performed comprehensive cMR with stress perfusion to evaluate the myocardial phenotype of 114 patients with Fabry disease pre-hypertrophy and pre-detectable storage. In pre-hypertrophic Fabry disease, a low T1 was associated with a constellation of ECG and functional abnormalities compared to normal T1 FD patients and controls. However, pre-hypertrophic Fabry disease patients with normal T1 also had abnormalities compared to controls: i.e. reduced GLS, lower microvascular changes as lower stress perfusion, subtle T2 elevation, and limited LGE. ECG abnormalities included shorter P-wave duration and T-wave peak time compared to controls. This supports a pre-LVH, pre-detectable storage phase of cardiac

involvement in Fabry disease characterized by subtle abnormalities of microvascular dysfunction, impaired LV mechanics, and altered atrial depolarization and ventricular repolarization intervals.<sup>32</sup>

Spath *et al.* evaluated a proof of concept study of Mg-enhanced cMR to evaluate calcium handling in dilated and hypertrophic cardiomyopathy. Manganese behaves as an analogue of calcium and is rapidly taken up by viable myocardium. Dynamic T1 mapping was performed before and every 2.5 min after IV injection of manganese dipyridoxyl diphosphate and the unidirectional influx constant  $K_i$  was determined in 17 patients with hypertrophic cardiomyopathy 10 with non-ischaemic dilated cardiomyopathy and 20 controls. In patients with dilated cardiomyopathy, manganese uptake rate correlated with LVEF. Rate of myocardial manganese uptake demonstrated stepwise reductions across healthy myocardium, hypertrophic cardiomyopathy without fibrosis, and hypertrophic cardiomyopathy with fibrosis providing absolute discrimination between the healthy myocardium and fibrosed myocardium<sup>33</sup> (Figure 1).

## Heart failure

In HF patients, LV GLS by 2D STE has a greater prognostic value than LVEF. Hwang *et al.* developed a mortality risk prediction model incorporating LV GLS in 1859 patients with acute HF retrospectively analysed from two centres (derivation cohort) and validated the model in 1389 patients from one centre (validation cohort). The model including clinical parameters [age, diabetes, body mass index, diastolic blood pressure, glomerular filtration rate, natriuretic peptide, and failure to prescribe beta-blockers and Renin angiotensin system (RAS) blockers] and LV GLS provided reliable prediction of the 2-year risk of mortality, suggesting its potential clinical usefulness in patients admitted for acute HF. The risk prediction model showed good performance not only in patients with HF<sub>r</sub>EF, but also in those with HF<sub>m</sub>rEF and HF<sub>p</sub>EF.<sup>34</sup>

Increased LV MD by 2D STE predicts ventricular arrhythmias in HF. Data from a prospective population-based cohort consisting of 2529 middle-aged subjects in Akershus County, Norway by Aagaard *et al.*<sup>35</sup> showed that coronary artery disease and hypertension were the strongest determinants of increased MD by STE. LV systolic and diastolic dysfunctions were also associated with increasing MD, albeit their relationship was weaker.

Blood biomarkers represent an easily accessible and rapid tool for HF diagnosis and prognosis. Klimczak-Tomaniak *et al.* looked at the relationship of the temporal changes of biomarkers and of echocardiographic parameters in 117 chronic HF patients with EF ≤50%. Among NT-proBNP, Hs-TnT, and CRP, only serial measurements of NT-proBNP independently reflected the changes in echocardiographic parameters of systolic function, LV filling pressures, estimated pulmonary pressure, and chamber dimensions. Notably, NT-proBNP appeared to reflect both disease progression on long term (e.g. gradual LVEF impairment, progressive chamber dilation) and more rapidly occurring haemodynamic changes (e.g. elevation in LV filling pressures).<sup>36</sup>

Detection of HF in a subclinical stage in patients at risk is highly desirable. Nishi *et al.* prospectively enrolled 161 asymptomatic patients with type 2 diabetes mellitus (DM) evaluated with echocardiography at rest and with exercise. They reported that diastolic stress testing

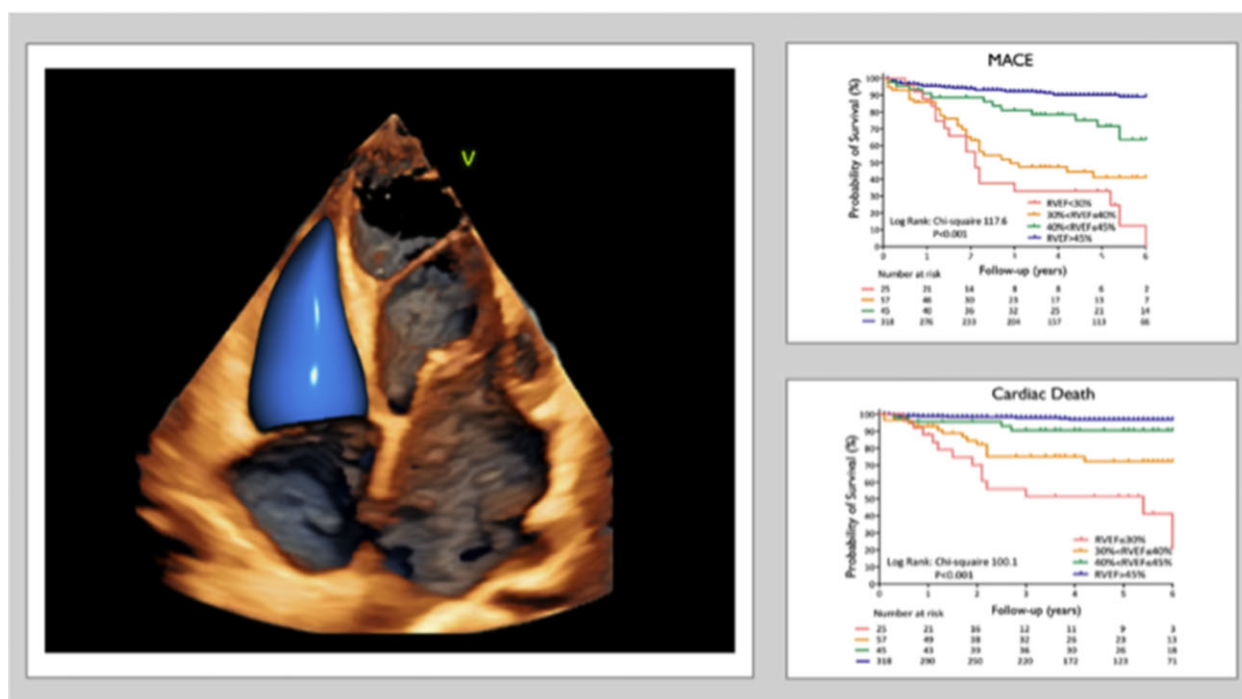


**Figure 1** Prognostic validation of partition values to grade right ventricular dysfunction severity. Kaplan–Meier estimates of survival to cardiac death (right panel), freedom from Major adverse cardiac events (MACE) and survival to all-cause mortality in the validation cohort using the new partition values to grade the severity of right ventricular dysfunction.

improved the detection of subclinical HF in patients with type 2 DM, with diastolic dysfunction revealed with exercise in 16% of these patients. Moreover, diastolic stress could delineate the mechanisms of exercise limitations in patients with DM.<sup>37</sup>

Ross *et al.* reported that septal contraction patterns revealed by STE are an excellent predictor of acute CRT response. They evaluated 39 CRT candidates grouped according to the presence or absence of septal dyssynchrony and evaluated the acute CRT response defined as  $\geq 10\%$  increase in LV  $dP/dt_{max}$  by invasive measurements, as well as positive changes in end-diastolic pressure and QRS width. Only CRT patients showing premature septal contraction by STE experienced acute systolic, diastolic, and electrical improvement under biventricular pacing.<sup>38</sup>

End-stage HF patients with LV assist device (LVAD) represent a challenge for transthoracic echocardiography, because of the extensive anatomic changes after device implantation and the interposition of hard implanted materials. Strachinaru *et al.* described a novel method to image difficult-to-scan LVAD patients using transhepatic echocardiography by right intercostal approach, allowing to obtain a four-chamber view. In 15 LVAD patients with very poor acoustic window, the transhepatic intercostal window was feasible in all patients, with good visualization of structures in 93%. This resulted in a higher rate of precise quantification of LV and RV function and of Doppler evaluation of LVAD inflow cannula.<sup>39</sup>

The prognostic role of RV strain to predict the risk for first hospitalization for HF and death of any cause was demonstrated by

Gavazzoni *et al.* in 458 asymptomatic patients with left-sided heart diseases. RV FWLS was able to predict outcome (best cut-off value  $-22\%$ ; AUC 0.677; sensitivity 70%; 65% specificity) and its prognostic value was maintained also in the subgroup of patients with normal TAPSE.<sup>40</sup>

Muraru *et al.* demonstrated that RVEF by 3D echocardiography holds an independent and superior prognostic value than conventional parameters of RV systolic function (e.g. TAPSE and fractional area change). In 412 consecutive patients with various heart diseases followed for  $3.7 \pm 1.4$  years (derivation cohort), they identified the partition values to define mild/moderate/severe RV dysfunction based on patient outcome. The partition values of 45%, 40%, and 30%, respectively, were validated in a separate cohort of 446 patients from a different centre, confirming the role of 3D RVEF to stratify the risk of cardiac death and Major adverse cardiac events (MACE) (Figure 2).<sup>41</sup>

Nuclear cardiology has a great role in the evaluation of the Morpho-metabolic post-surgical patterns of infected and non-infected prosthetic heart valves (PVs). Roque and Coll evaluated a series of 37 post-operative patients to define characteristic positron emission tomography/computed tomography angiography (CTA) patterns of Fluorodesoxyglucose (FDG) uptake and anatomic changes following PVs implantation over time, in order to help not to misdiagnose post-operative inflammation and avoid false-positive cases. The authors concluded that FDG uptake, often seen in recently implanted PVs, shows a characteristic pattern of post-operative inflammation and, in the absence of associated anatomic lesions, could



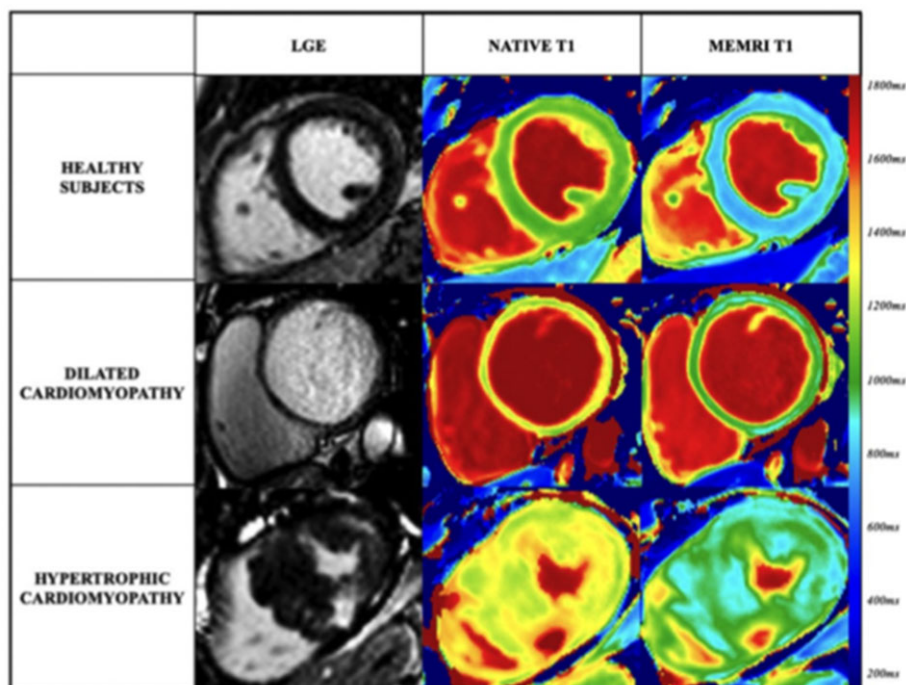


**Figure 2** Late gadolinium-enhanced, native T1 and manganese-enhanced magnetic resonance imaging in healthy volunteers and patients with non-ischaemic cardiomyopathy. Representative late gadolinium enhancement, native and manganese-enhanced magnetic resonance imaging T1 mapping in (A) healthy volunteer, (B) patient with dilated cardiomyopathy, and (C) patient with hypertrophic cardiomyopathy following manganese dipyridoxyl diphosphate infusion.

be considered a normal finding. These features remain stable for at least 1 year after surgery, so questioning the recommended 3-month safety period, demonstrating that in patients with suspected infection of PVs, nuclear cardiology can be of help in the clinical management.<sup>42</sup>

Another interesting use of computed tomography (CT) in HF patients has been shown by Colin and Coll. The authors evaluated the relationships between pulmonary transit time (PTT), cardiac function, and pulmonary haemodynamics in 57 patients with HFrEF and explored how PTT performs in detecting pulmonary hypertension (PH). The authors concluded that PTT correlates with cardiac function and pulmonary haemodynamics is determined by four independent parameters [pulmonary artery wedge pressure, cardiac index, mitral regurgitation (MR) grade, and RV end-diastolic volume] and performs well in detecting PH.<sup>43</sup>

## Congenital heart disease

Moceri *et al.* prospectively evaluated adolescents and adults with atrial septal defect (ASD,  $n = 27$ ) and tetralogy of Fallot (TOF,  $n = 28$ ) with chronic pulmonic regurgitation. A rigorous examination of the right ventricle, including local and global 3D deformation and curvature analyses showed that chronic RV volume loading results in similar RV shape remodelling in both ASD and TOF patients. However,

TOF patients have more hypertrophic RV, reduced systolic function, and strain as compared to ASD patients in whom both longitudinal and circumferential strains are preserved. The conclusion was that left-to-right atrial shunt and pulmonic regurgitation are responsible for different types of RV remodelling.<sup>44</sup>

Gupta *et al.* investigated the anatomy of a common arterial trunk, a rare cardiac malformation, in a series of 70 patients to clarify anatomic variations with the use of echocardiography and multidetector computed tomography (MDCT). The study shed light on different components of this complex congenital lesion including truncal valvar morphology, pulmonary circulation, pulmonary stenosis, coronary circulation, aortic arch and arch vessels, and other associated anomalies such as ASD. A wide variability in the arrangement of the pulmonary and coronary arterial components was reported. Aortic dominance was common. These morphological findings have important implications for individualized management of the patients.<sup>45</sup>

Rodriguez-Granillo *et al.* addressed the impact of pectus excavatum on cardiac morphology and function, according to the site of maximum compression, using multimodality imaging. Patients with compression affecting the right ventricle and atrioventricular block (AV) groove manifested exercise symptoms; stress-related signs of diastolic dysfunction and/or increased transtricuspid gradient; systolic dysfunction; inspiratory septal flattening; and/or mild pericardial effusion. The extent of these alterations was related to the site of

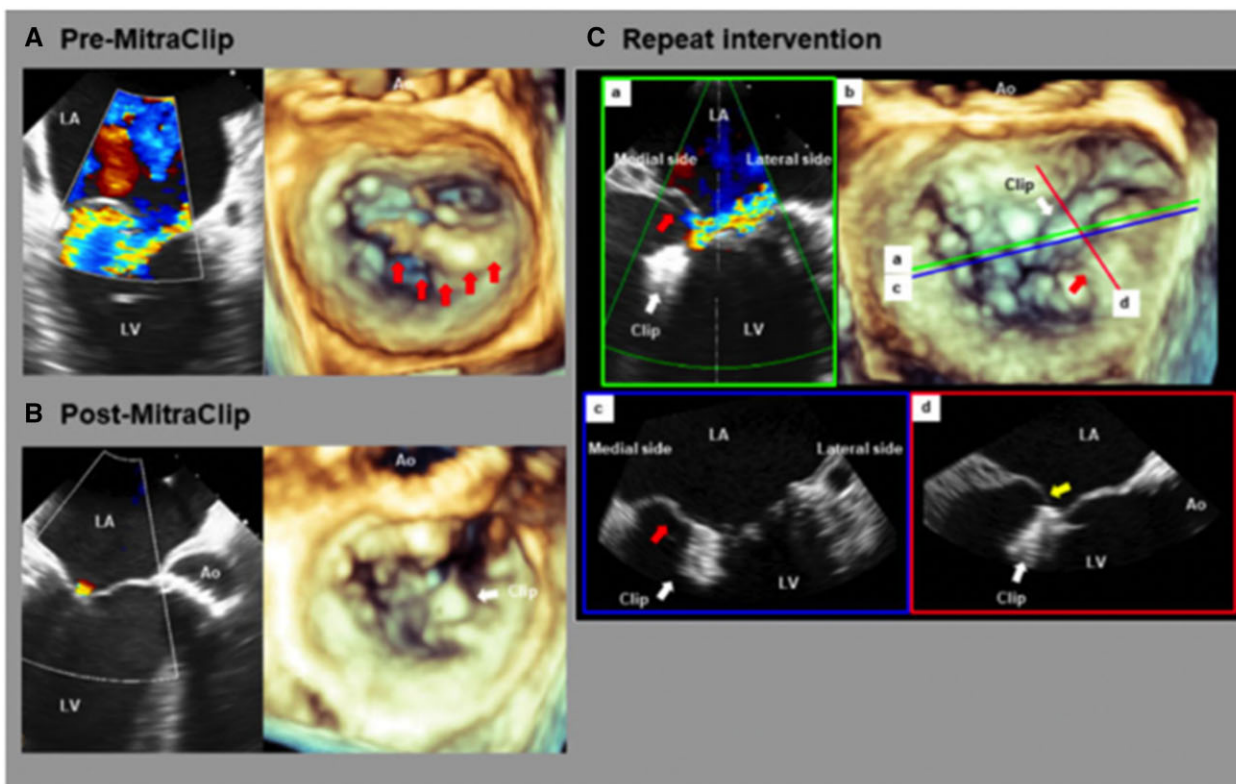


**Figure 3** TOE images of recurrent MR derived from worsening prolapse without a leaflet tear. (A) Pre-MitraClip. Red arrows indicate severe prolapse of P3 segment. (B) Post-MitraClip. White arrow indicates implanted clip. After one clip was implanted on A3–P3 segment, the grade of MR was reduced from severe to mild. (C) Repeat intervention. One clip was attached. However, prolapse on P2–P3 segment was worsening (red arrow in A–C). Yellow arrow indicates leaflet/clip connection (D). Ao, aortic valve; LA, left atrium; LV, left ventricle; MR, mitral regurgitation; TOE, transoesophageal echocardiography.

maximum compression over the right heart cavities. These data are of added value to critical thresholds for surgical correction.<sup>46</sup>

## Valvular heart disease

### Mitral regurgitation

Ikenaga *et al.* investigated morphological changes that are leading to repeat interventions for recurrent MR after initial MitraClip procedures, by using 3D transoesophageal echocardiography. Worsening prolapse at the clip site was the most frequent cause of recurrent MR among primary MR patients followed by leaflet tear at the clip site. In secondary MR, the progression of LV remodelling with increasing leaflet tenting was the most frequent cause of recurrence. Number of clips was not predictor. Meanwhile device detachment was observed more frequently in patients with primary MR<sup>47</sup> (Figure 3).

Recent studies showed that after implantation of a semi-rigid ring with a fixed orifice functional mitral valve area (MVA) is dynamic during exercise in association with diastolic anterior leaflet tethering. Accordingly, Petrus *et al.* assessed exercise haemodynamics after restrictive mitral annuloplasty for functional MR in patients ( $n=32$ )

who received smallest ring sizes available (no 24 and 26). MVA decreased, instead of increasing in 7 out of 32 patients during exercise. This was associated with a higher increase in mean pulmonary artery pressure with respect to cardiac output, absence of LV reverse remodelling, and worse survival even in the absence of recurrent MR.<sup>48</sup>

Bartko *et al.* casted the assessment of functional regurgitant lesions in the failing heart as an outcome predictor. They studied 414 patients with 5-year follow-up for all-cause mortality. The sum of mitral and tricuspid regurgitant volume of  $\geq 50$  mL/beat was associated with more remodelling and steadily increasing risk of mortality after this threshold, suggesting a transition from HF to valvular-driven HF progression. These data arise the question whether two moderate lesions should be treated considering the advances in low-risk transcatheter repair techniques.<sup>49</sup>

Gavazzoni *et al.*<sup>50</sup> published a comprehensive review elaborating on the treatment strategies of complex and challenging mitral valve lesions by MitraClip where they described special considerations for echocardiographic guidance.

## Aortic valve

Kebed *et al.* revisited echo criteria for the classification of severe aortic stenosis (AS) in a retrospective cohort of 916 patients. They showed that the constellation of aortic valve area (AVA)  $<1 \text{ cm}^2$ ,  $V_{\text{max}} \geq 4 \text{ m/s}$ , or  $\Delta P \geq 40 \text{ mmHg}$  for severe AS is internally inconsistent in  $\sim 30\%$  of cases even in the setting of normal LV systolic function. The investigators demonstrated race and gender-related differences in AS progression and provided alternative cut-offs: AVA =  $1 \text{ cm}^2$  corresponded to mean gradient of 32 mmHg and  $V_{\text{max}} = 3.7 \text{ m/s}$ , while mean gradient of 40 mmHg corresponded to AVA =  $0.89 \text{ cm}^2$ .<sup>51</sup>

Shen *et al.* studied the aortic valve phenotype on haemodynamic and anatomic progression of AS in 141 participants with mild to moderate AS, (32 with bicuspid aortic valve; BAV, 109 with tricuspid aortic valve; TAV) over 2 years. Echo Doppler was used for haemodynamic assessment and CT for aortic valve calcification (AVC). After adjustment for age, baseline stenosis severity, and several risk factors (i.e. sex, history of hypertension, creatinine level, diabetes, metabolic syndrome), BAV was independently associated with faster anatomic and haemodynamic progression and higher risk of AVR or death, when compared with TAV. In subjects with TAV, progression of AS was mainly driven by cardiometabolic risk factors, whereas in BAV subjects, genetic predisposition and abnormal valve morphology appeared to have an independent contribution to AS progression.<sup>52</sup>

Kong *et al.* evaluated the proportion and prognostic value of impaired LV GLS in 513 patients with BAV and preserved EF. LV GLS  $-13.6\%$  was an event predictor (mainly aortic valve replacement) independently of type and severity of valve dysfunction. These data are consolidating the existing body of evidence on the importance of GLS for risk stratification.<sup>53</sup> Furthermore, Ilardi *et al.* showed that endocardial strain outperformed other layers in a layer-specific approach, to predict cardiovascular death, particularly in symptomatic patients. Notably, the best endocardial strain value associated with outcome was  $-20.6\%$ , yet with moderate accuracy.<sup>54</sup>

Vollema *et al.* showed the incremental value of LV GLS on top of the proposed staging classification of cardiac damage in 616 patients with severe AS. LV GLS was divided by quintiles and assigned to the different stages. The endpoint was all-cause mortality. Over a median follow-up of 44 (24–89) months, 234 (38%) patients died. Incorporation of LV GLS by quintiles in novel proposed staging classification resulted in refinement of risk stratification by identifying patients with more advanced cardiac damage, improved the prognostic value of the originally proposed staging classification.<sup>55</sup>

Given the limitations of EF, research for better defining LV function has been focused not only on GLS but also on diastolic indices. Anand *et al.* investigated LV diastolic stiffness in patients with severe AS undergoing AVR. By a retrospective non-invasive assessment including 1893 patients, they were able to show that the association of LV chamber stiffening with mortality was present for each grade of diastolic dysfunction in both preserved and reduced EF subsets.<sup>56</sup>

Kellermaier *et al.* studied high molecular weight von Willebrand Factor deficiency as a rapid shear flow sensor to help the diagnosis of true stenotic low-flow/low-gradient (LF/LG) AS. The multimer deficiency correlates with transvalvular gradients and wall shear stress. Therefore, multimer deficiency occurred in patients having true-

severe LF/LG AS and contractile reserve but not those having pseudo severe LF/LG AS. In 30% of patients, further diagnostic testing could be avoided with the help of a multimer pattern. Multimer deficiency can complement indeterminate dobutamine stress echo results and help to reduce further testing.<sup>57</sup>

The integration of energy loss index (ELI) to circumvent the impact of pressure recovery on miscalculation of AVA by the continuity equation was tested in two clinical studies: Altes *et al.* tested the use of ELI in patients with LG severe AS with preserved LVEF. Almost 40% of patients were reclassified as having moderate AS by ELI: aortic valve area indexed (AVA<sub>i</sub>)  $<0.6 \text{ cm}^2/\text{m}^2$  but an ELI  $>0.6 \text{ cm}^2/\text{m}^2$ . Reclassification as moderate AS by ELI was associated with reduced need for surgery and reduced rate of mortality during follow-up compared with patients who were not reclassified. Hence, these results support the potential interest of calculating ELI in routine practice in patients with discordant measurements for severe AS and preserved LVEF.<sup>58</sup> In another study, Holy *et al.* retrospectively included 197 patients undergoing TAVI. The authors used a fused method incorporating MDCT derived planimetric areas of sinotubular junction and LV outflow tract (LVOT) with TTE Doppler measurements to estimate AVA<sub>i</sub> and ELI. Although the circular anatomy of the sinotubular junction yielded similar area measurements with TTE and MDCT, LVOT area driven from diameter by TTE consistently underestimated the LVOT planimetric area by MDCT. Planimetered area for LVOT was used in the calculation of fusion ELI. Forty-three percent of patients initially diagnosed with severe AS were reclassified to moderate AS. Of note, reclassification occurred mostly in patients categorized as normal-flow LG AS. TAVI resulted in a similar functional improvement of both reclassified patients and those with true-severe AS. The reclassified group displayed lower rates of all-cause mortality at 3-year follow-up, suggesting that TAVI may be a valuable therapeutic strategy also in symptomatic patients with moderate or borderline moderate-to-severe AS.<sup>59</sup>

EACVI scientific initiatives committee led a survey on the evaluation of AS that shedded light on how the new guidelines are implemented across Europe from the perspective of the use and access of advanced imaging techniques in AS.<sup>12</sup>

Regarding possible risk factors that can impact on AVC, Sønderkov and Coll aimed to clarify if patients on vitamin K antagonist (VKA) treatment, the most frequently prescribed anticoagulant worldwide, have increased AVC score compared with patients treated with the new oral anticoagulants (NOAC) and patients who never treated with VKA or NOAC. The final population consisted of 14 604 participants (67.4 years, 95% men) of whom 873 had been treated with VKA and 602 with NOAC. The results were consistent in sensitivity analyses excluding patients with known cardiovascular disease and statin users. Compared to no treatment with anticoagulants, VKA use was associated with increased AVC score, while a similar association could not be established for NOAC.<sup>60</sup>

Also in valvular heart disease Postigo *et al.* compared the clinical efficacy of echocardiography and cMR in 263 consecutive patients with isolated aortic regurgitation undergoing both tests to reach a primary endpoint of HF or valve surgery. cMR-derived regurgitant fraction and LV end-diastolic volume adequately stratified patients with normal EF and adjusted survival models based on cMR improved the predictions of the primary endpoint based on echocardiography with significant reclassification index.<sup>61</sup>



## Prosthetic valves

Vriesendorp *et al.* tested whether projected prosthesis–patient mismatch (PPM) derived from indexed effective orifice area (EOAi) charts, accurately predict measured PPM, in the population ( $n = 996$ ) derived from the PERIcarial SurGical Aortic Valve Replacement (PERIGON) Pivotal Trial. Measured EOA plotted against projected EOAi showed a weak correlation ( $r = 0.53$ ) and low specificity (37%) to predict PPM. The use of an EOAi chart led to the incorrect prediction of PPM in 22% of the patients, the rate of misclassification increased to 45% for the valve size 19 mm, whereas the inaccuracy was 9% for the valve size 27 mm. This misclassification questions the use of EOAi reference charts for valve selection, for decision-making about annular enlargement before valve implantation and finally for examining the effect of PPM on the outcome. The authors recommended the use of measured instead of projected EOAi to study the impact of PPM on outcomes.<sup>62</sup>

Winter *et al.* studied the evolution of concomitant secondary mitral and tricuspid regurgitation after transcatheter aortic valve replacement (TAVR) in prospectively enrolled 429 consecutive patients by echo on a yearly basis after TAVR. Severe secondary MR regressed in 59% whereas secondary tricuspid regurgitation (TR) regressed in 43% of patients. Persistence of atrioventricular regurgitations was associated with excess long-term mortality, whereas post-TAVR reduction of atrioventricular regurgitation resulted in mortality rates comparable to those seen in patients without concomitant secondary regurgitation. Of note, rheumatic and myxomatous valve diseases were excluded. The results suggest early staged reintervention for the concomitant valvular lesions in case of persistence to mitigate excess mortality risk.<sup>63</sup>

Okuno *et al.* showed that isolated severe mitral annular calcification (MAC) in the absence of mitral valve disease (MVD) has no effect on clinical outcomes following TAVR in patients with preserved mitral valve function. Yet, patients with MVD had an increased risk of death at 1 year irrespective of MAC.<sup>64</sup>

Stella *et al.* published their large experience on the intra-procedural monitoring protocol using routine TTE with backup TOE for TAVR. They showed that TTE does not cause delays in diagnosing complications and reliably detects paravalvular leaks. Omitting TOE as a continuous imaging tool during TAVR, and adopting TTE with conscious sedation does not seem to affect procedural success in experienced centres.<sup>65</sup>

In valvular heart disease, the important role of cMR RV function assessment was demonstrated by a study by Koschutnik *et al.* who compared the prognostic value of RV parameters by echocardiography [Tricuspid annular plane systolic excursion (TAPSE), Fractional area change (FAC), RV free wall Doppler  $S'$ , and strain] vs. RVEF by cMR in 204 patients undergoing TAVR for AS. All RV function parameters were found to be associated with NT-proBNP levels, but only FAC and RVEF were significantly associated with a prolonged in-hospital stay. Patients were followed over a mean of 13 months for death or hospitalization for HF. After adjustment for the EuroSCORE II, only cMR-derived RVEF was significantly associated with the composite endpoint. In contrast, RVD dysfunction as defined by echocardiography failed to predict outcomes after adjustment for pre-existing clinical risk factors in TAVR patients.<sup>66</sup>

The detection of cardiac valvular calcification on routine imaging may provide an opportunity to identify individuals at increased risk for peripheral artery disease (PAD). Garg and Coll investigated the associations of AVC and MAC (MAC) with risk of developing clinical PAD or a low ankle–brachial index (ABI). AVC and MAC were measured on cardiac CT in 6778 Multi-Ethnic Study of Atherosclerosis participants without baseline PAD. There were 117 clinical PAD and 198 low ABI events that occurred over a median follow-up of 14 and 9.2 years, respectively. The authors concluded that MAC is associated with an increased risk of developing clinical PAD, even if future studies are needed to corroborate these findings.<sup>67</sup>

## Tricuspid regurgitation

Chorin *et al.* evaluated the impact of TR severity on HF hospitalization and mortality in a retrospective study by semi-quantitative analyses from consecutive echocardiograms ( $n = 33\,305$ ). Any degree of TR (1-year mortality rates 7.7%, 16.8%, 29.5%, and 45.6% in no, mild, moderate, and severe TR, respectively) was associated with adverse clinical outcome after adjusting for age, sex, LVEF, other heart valve diseases, or PH. The study supports an aggressive approach to treatment of secondary TR.<sup>68</sup>

In another retrospective study including 676 patients with all-cause TR, Peri *et al.* showed that quantitative assessment of TR by effective regurgitant orifice area measurement is a powerful independent predictor of outcome, superior to standard qualitative assessment. Torrential TR with effective orifice area  $>0.7\text{ cm}^2$  was associated with poorer survival than severe TR ( $>0.4\text{ cm}^2$ ) in support of another threshold for extreme risk (torrential/massive TR) in TR grading.<sup>69</sup>

Ortiz-Leon *et al.* used a novel automated dedicated tricuspid valve (TV) software and compared TV geometry in groups having AF only, AF associated with left heart disease vs. controls. Inter- and intra-observer variabilities showed strong agreement for all tricuspid annulus (TA) measurements except for TA end-diastolic minimum diameter. The study added another important contribution to the body of knowledge by showing that AF is associated with right atrial and TA remodelling independently from left heart disease. The study also showed the feasibility and accuracy of a new software for measuring and defining 3D anatomy of TV, annulus, and right heart chambers.<sup>70</sup>

Utsunomiya *et al.* showed that right heart remodelling and TV geometry differ between atrial and ventricular functional TR. In atrial functional TR, geometric changes of the TA depend on right atrial enlargement; whereas geometric changes of the tricuspid leaflets mainly depend on relative positional relationship between each papillary muscle tip and the centre of TA. In contrast, ventricular functional TR is determined by leaflet tethering and tenting linked to RV spherical deformation. Torrential atrial functional TR on the other hand is characterized by significant tethering on top of prominent annular dilatation and large gap between the leaflet edges. These findings have therapeutic implications.<sup>71</sup>

## Emerging techniques

One of the major strengths of cMR is its ability to assess multiple parameters, such as cardiac function, inflammation, and oedema through T1 and T2 imaging and mapping and injury through LGE.



Galea *et al.*<sup>72</sup> proposed a combined cardiothoracic magnetic resonance imaging protocol, that could provide a ‘one stop-shop’ evaluation of cardiovascular structures, lung parenchyma, and pulmonary arterial tree, in COVID-19 patients with progressive worsening of clinical conditions and/or suspicion of acute-onset myocardial inflammation.

Finally, several studies proposed new cMR techniques. Larsen *et al.* evaluated the feasibility of the estimation of regional myocardial work from strain by feature tracking cardiac magnetic resonance and non-invasive LV pressure estimation in 37 HF patients with reduced EF, and left bundle branch block and 9 controls. In left bundle branch block, segmental work was reduced in septum relative to lateral work, whereas it was homogeneous in controls. Segmental cMR-derived work correlated with segmental STE-derived work and with energy demand as reflected in segmental FDG uptake. These results suggest that FT-cMR in combination with non-invasive left ventricular pressure (LVP) is a relevant clinical tool to measure regional myocardial work.<sup>73</sup> Bhuva *et al.* proposed combining cMR phase contrast and brachial suprasystolic wave oscillometry to perform wave intensity analysis in the aorta and to evaluate ventriculoarterial coupling. The temporal resolution was sufficiently high to demonstrate ageing and female sex was independently associated with decreased forward compression wave (FCW) energy and an increased proportion of wave reflection, suggesting a less energy efficient cardiovascular system.<sup>74</sup>

**Conflict of interest:** none declared.

## References

- Edvardsen T, Haugaa KH, Petersen SE, Gimelli A, Donal E, Maurer G *et al.* The year 2019 in the European Heart Journal—Cardiovascular Imaging: part I. *Eur Heart J Cardiovasc Imaging* 2020;**21**:1208–15.
- Cosyns B, Haugaa KH, Gerber B, Gimelli A, Sade LE, Maurer G *et al.* The year 2019 in the European Heart Journal—Cardiovascular Imaging: part II. *Eur Heart J Cardiovasc Imaging* 2021;**21**:1331–40.
- Slart RHJA, Glaudemans AWJM, Gheysens O, Lubberink M, Kero T, Dweck MR *et al.* 4Is Cardiovascular Imaging: a joint initiative of the European Association of Cardiovascular Imaging (EACVI) and the European Association of Nuclear Medicine (EANM). Procedural recommendations of cardiac PET/CT imaging: standardization in inflammatory-, infective-, infiltrative-, and innervation- (4Is) related cardiovascular diseases: a joint collaboration of the EACVI and the EANM: summary. *Eur Heart J Cardiovasc Imaging* 2021;**21**:1320–30.
- Dweck MR, Maurovich-Horvat P, Leiner T, Cosyns B, Fayad ZA, Gijzen FJH *et al.* Contemporary rationale for non-invasive imaging of adverse coronary plaque features to identify the vulnerable patient: a position paper from the European Society of Cardiology Working Group on Atherosclerosis and Vascular Biology and the European Association of Cardiovascular Imaging. *Eur Heart J Cardiovasc Imaging* 2020;**21**:1177–83.
- Citro R, Okura H, Ghadri JR, Izumi C, Meimoun P, Izumo M *et al.*; EACVI Scientific Documents Committee. Multimodality imaging in takotsubo syndrome: a joint consensus document of the European Association of Cardiovascular Imaging (EACVI) and the Japanese Society of Echocardiography (JSE). *Eur Heart J Cardiovasc Imaging* 2020;**21**:1184–207.
- Popescu BA, Stefanidis A, Fox KF, Cosyns B, Delgado V, Di Salvo G *et al.*; Reviewers: This document was reviewed by members of the 2018–2020 EACVI Scientific Documents Committee: Philippe Bertrand, Marc Dweck, Bernhard Gerber, Ivan Stankovic. Training, competence, and quality improvement in echocardiography: the European Association of Cardiovascular Imaging Recommendations: update 2020. *Eur Heart J Cardiovasc Imaging* 2021;**21**:1305–19.
- Skulstad H, Cosyns B, Popescu BA, Galderisi M, Di Salvo G, Donal E *et al.* COVID-19 pandemic and cardiac imaging: EACVI recommendations on precautions, indications, prioritization, and protection for patients and healthcare personnel. *Eur Heart J Cardiovasc Imaging* 2020;**21**:592–8.
- Cosyns B, Lochy S, Luchian ML, Gimelli A, Pontone G, Allard SD *et al.* The role of cardiovascular imaging for myocardial injury in hospitalized COVID-19 patients. *Eur Heart J Cardiovasc Imaging* 2020;**21**:709–14.
- Gargani L, Soliman-Aboumarie H, Volpicelli G, Corradi F, Pastore MC, Cameli M. Why, when, and how to use lung ultrasound during the COVID-19 pandemic: enthusiasm and caution. *Eur Heart J Cardiovasc Imaging* 2020;**21**:941–8.
- Dweck MR, Bularga A, Hahn RT, Bing R, Lee KK, Chapman AR *et al.* Global evaluation of echocardiography in patients with COVID-19. *Eur Heart J Cardiovasc Imaging* 2020;**21**:949–58.
- Holte E, Dweck MR, Marsan NA, D’Andrea A, Manka R, Stankovic I *et al.* EACVI survey on the evaluation of infective endocarditis. *Eur Heart J Cardiovasc Imaging* 2020;**21**:828–32.
- Michalski B, Dweck MR, Marsan NA, Cameli M, D’Andrea A, Carvalho RF *et al.* The evaluation of aortic stenosis, how the new guidelines are implemented across Europe: a survey by EACVI. *Eur Heart J Cardiovasc Imaging* 2020;**21**:357–62.
- Ajmone Marsan N, Michalski B, Cameli M, Podlesnikar T, Manka R, Sitges M *et al.* EACVI survey on standardization of cardiac chambers quantification by transthoracic echocardiography. *Eur Heart J Cardiovasc Imaging* 2020;**21**:119–23.
- Voigt J-U, Mălăescu G-G, Haugaa K, Badano L. How to do la strain. *Eur Heart J Cardiovasc Imaging* 2020;**21**:715–7.
- Badano LP, Muraru D, Parati G, Haugaa K, Voigt JU. How to do right ventricular strain. *Eur Heart J Cardiovasc Imaging* 2020;**21**:825–7.
- Hyafil F, Jaber WA, Neglia D. Highlights of the 14th international conference on nuclear cardiology and cardiac computed tomography. *Eur Heart J Cardiovasc Imaging* 2020;**21**:1–9.
- Rodriguez-Palomares JF, Edvardsen T, Almeida AG, Petersen SE. EuroCMR 2019 highlights. *Eur Heart J Cardiovasc Imaging* 2020;**21**:127–31.
- Magne J, Bharucha T, Cikes M, Galderisi M, Price S, Sade LE *et al.* EuroEcho 2019: highlights. *Eur Heart J Cardiovasc Imaging* 2020;**21**:469–78.
- Baudry G, Mansencal N, Reynaud A, Richard P, Dubourg O, Komajda M *et al.* Global and regional echocardiographic strain to assess the early phase of hypertrophic cardiomyopathy due to sarcomeric mutations. *Eur Heart J Cardiovasc Imaging* 2020;**21**:291–8.
- Jurlander R, Mills HL, Espersen KI, Raja AA, Svendsen JH, Theilade J *et al.* Screening relatives in arrhythmogenic right ventricular cardiomyopathy: yield of imaging and electrical investigations. *Eur Heart J Cardiovasc Imaging* 2020;**21**:175–82.
- Nicol M, Baudet M, Brun S, Harel S, Royer B, Vignon M *et al.* Diagnostic score of cardiac involvement in AL amyloidosis. *Eur Heart J Cardiovasc Imaging* 2020;**21**:542–8.
- Brand A, Frumkin D, Hübscher A, Dreger H, Stangl K, Baldenhofer G *et al.* Phasic left atrial strain analysis to discriminate cardiac amyloidosis in patients with unclear thick heart pathology. *Eur Heart J Cardiovasc Imaging* 2021;**22**:680–7.
- Clemmensen TS, Eiskjær H, Ladefoged B, Mikkelsen F, Sørensen J, Granstam SO *et al.* Prognostic implications of left ventricular myocardial work indices in cardiac amyloidosis. *Eur Heart J Cardiovasc Imaging* 2021;**22**:695–704.
- Kusunose K, Fujiwara M, Yamada H, Nishio S, Saijo Y, Yamada N *et al.* Deterioration of biventricular strain is an early marker of cardiac involvement in confirmed sarcoidosis. *Eur Heart J Cardiovasc Imaging* 2020;**21**:796–804.
- Jurcuț R, Onciul S, Adam R, Stan C, Coriu D, Rapezzi C *et al.* Multimodality imaging in cardiac amyloidosis: a primer for cardiologists. *Eur Heart J Cardiovasc Imaging* 2020;**21**:833–44.
- Abou R, Prihadi EA, Goedemans L, Van Der Geest R, El Mahdoui M, Schaliq MJ *et al.* Left ventricular mechanical dispersion in ischaemic cardiomyopathy: association with myocardial scar burden and prognostic implications. *Eur Heart J Cardiovasc Imaging* 2020;**21**:1227–34.
- Pagourelas ED, Mirea O, Duchenne J, Unlu S, Van Cleemput J, Papadopoulos CE *et al.* Speckle tracking deformation imaging to detect regional fibrosis in hypertrophic cardiomyopathy: a comparison between 2D and 3D echo modalities. *Eur Heart J Cardiovasc Imaging* 2020;**21**:1262–72.
- Hooks M, Okasha O, Velangi PS, Nijjar PS, Farzaneh-Far A, Shenoy C. Left ventricular thrombus on cardiovascular magnetic resonance imaging in non-ischaemic cardiomyopathy. *Eur Heart J Cardiovasc Imaging* 2020;jeaa244.doi: 10.1093/ehjci/jeaa244.
- Xu Y, Lin J, Liang Y, Wan K, Li W, Wang J *et al.* Prognostic value of left ventricular remodelling index in idiopathic dilated cardiomyopathy. *Eur Heart J Cardiovasc Imaging* 2021;**22**:1197–207.
- Putko BN, Savu A, Kaul P, Ezekowitz J, Dyck JR, Anderson TJ *et al.* Left atrial remodelling, mid-regional pro-atrial natriuretic peptide, and prognosis across a range of ejection fractions in heart failure. *Eur Heart J Cardiovasc Imaging* 2021;**22**:220–8.
- Yang K, Song YY, Chen XY, Wang JX, Li L, Yin G *et al.* Apical hypertrophic cardiomyopathy with left ventricular apical aneurysm: prevalence, cardiac magnetic resonance characteristics, and prognosis. *Eur Heart J Cardiovasc Imaging* 2021;**21**:1341–50.
- Augusto JB, Eiros R, Nakou E, Moura-Ferreira S, Treibel TA, Captur G *et al.* Dilated cardiomyopathy and arrhythmogenic left ventricular cardiomyopathy: a

- comprehensive genotype-imaging phenotype study. *Eur Heart J Cardiovasc Imaging* 2020;**21**:326–36.
33. Spath NB, Singh T, Papanastasiou G, Kershaw L, Baker AH, Janiczek RL et al. Manganese-enhanced magnetic resonance imaging in dilated cardiomyopathy and hypertrophic cardiomyopathy. *Eur Heart J Cardiovasc Imaging* 2020;jeaa273.doi: 10.1093/ehjci/jeaa273.
  34. Hwang IC, Cho GY, Choi HM, Yoon YE, Park JJ, Park JB et al. Derivation and validation of a mortality risk prediction model using global longitudinal strain in patients with acute heart failure. *Eur Heart J Cardiovasc Imaging* 2020;**21**:1412–20.
  35. Aagaard EN, Kvisvik B, Pervez MO, Lyngbakken MN, Berge T, Enger S et al. Left ventricular mechanical dispersion in a general population: data from the Akershus Cardiac Examination 1950 study. *Eur Heart J Cardiovasc Imaging* 2020;**21**:183–90.
  36. Klimczak-Tomaniak D, van den Berg VJ, Strachinaru M, Martijn Akkerhuis K, Baart S, Caliskan K et al. Longitudinal patterns of N-terminal pro B-type natriuretic peptide, troponin T, and C-reactive protein in relation to the dynamics of echocardiographic parameters in heart failure patients. *Eur Heart J Cardiovasc Imaging* 2020;**21**:1005–12.
  37. Nishi T, Kobayashi Y, Christle JW, Cauwenberghs N, Boralkar K, Moneghetti K et al. Incremental value of diastolic stress test in identifying subclinical heart failure in patients with diabetes mellitus. *Eur Heart J Cardiovasc Imaging* 2020;**21**:876–84.
  38. Ross S, Nestaas E, Kongsgaard E, Odland HH, Haland TF, Hopp E et al. Septal contraction predicts acute haemodynamic improvement and paced QRS width reduction in cardiac resynchronization therapy. *Eur Heart J Cardiovasc Imaging* 2020;**21**:845–52.
  39. Strachinaru M, Bowen DJ, Constatinescu A, Manintveld OC, Brugs J, Geleijnse ML et al. Transhepatic echocardiography: a novel approach for imaging in left ventricle assist device patients with difficult acoustic windows. *Eur Heart J Cardiovasc Imaging* 2020;**21**:491–7.
  40. Gavazzoni M, Badano LP, Vizzardi E, Raddino R, Genovese D, Taramasso M et al. Prognostic value of right ventricular free wall longitudinal strain in a large cohort of outpatients with left-side heart disease. *Eur Heart J Cardiovasc Imaging* 2020;**21**:1013–21.
  41. Muraru D, Badano LP, Nagata Y, Surkova E, Nabeshima Y, Genovese D et al. Development and prognostic validation of partition values to grade right ventricular dysfunction severity using 3D echocardiography. *Eur Heart J Cardiovasc Imaging* 2020;**21**:10–21.
  42. Roque A, Pizzi MN, Fernández-Hidalgo N, Permanyer E, Cuellar-Calabria H, Romero-Farina G et al. Morpho-metabolic post-surgical patterns of non-infected prosthetic heart valves by [18F]FDG PET/CTA: “normality” is a possible diagnosis. *Eur Heart J Cardiovasc Imaging* 2020;**21**:24–33.
  43. Colin GC, Pouleur AC, Gerber BL, Poncellet PA, De Meester C, D'Hondt AM et al. Pulmonary hypertension detection by computed tomography pulmonary transit time in heart failure with reduced ejection fraction. *Eur Heart J Cardiovasc Imaging* 2020;**21**:1291–8.
  44. Mocerri P, Duchateau N, Gillon S, Jaunay L, Baudouy D, Squara F et al. Three-dimensional right ventricular shape and strain in congenital heart disease patients with right ventricular chronic volume loading. *Eur Heart J Cardiovasc Imaging* 2021;**22**:1174–81.
  45. Gupta SK, Aggarwal A, Shaw M, Gulati GS, Kothari SS, Ramakrishnan S et al. Clarifying the anatomy of common arterial trunk: a clinical study of 70 patients. *Eur Heart J Cardiovasc Imaging* 2020;**21**:914–22.
  46. Rodriguez-Granillo GA, Raggio IM, Deviggiano A, Bellia-Munzon G, Capunay C, Nazzari M et al. Impact of pectus excavatum on cardiac morphology and function according to the site of maximum compression: Effect of physical exertion and respiratory cycle. *Eur Heart J Cardiovasc Imaging* 2020;**21**:44–84.
  47. Ikenaga H, Makar M, Rader F, Siegel RJ, Kar S, Makkar RR et al. Mechanisms of mitral regurgitation after percutaneous mitral valve repair with the MitraClip. *Eur Heart J Cardiovasc Imaging* 2020;**21**:1131–43.
  48. Petrus AHJ, Tops LF, Holman ER, Marsan NA, Bax JJ, Schalij MJ et al. Exercise haemodynamics after restrictive mitral annuloplasty for functional mitral regurgitation. *Eur Heart J Cardiovasc Imaging* 2020;**21**:299–306.
  49. Bartko PE, Arfsten H, Heitzinger G, Pavo N, Spinka G, Kastl S et al. Global regurgitant volume: approaching the critical mass in valvular-driven heart failure. *Eur Heart J Cardiovasc Imaging* 2020;**21**:168–74.
  50. Gavazzoni M, Taramasso M, Zuber M, Russo G, Pozzoli A, Miura M et al. Conceiving MitraClip as a tool: percutaneous edge-to-edge repair in complex mitral valve anatomies. *Eur Heart J Cardiovasc Imaging* 2020;**21**:1059–67.
  51. Kebed K, Sun D, Addetia K, Mor-Avi V, Markuzon N, Lang RM. Progression of aortic stenosis and echocardiographic criteria for its severity. *Eur Heart J Cardiovasc Imaging* 2020;**21**:737–43.
  52. Shen M, Tastet L, Capoulade R, Arsenaault M, Bedard E, Clavel MA et al. Effect of bicuspid aortic valve phenotype on progression of aortic stenosis. *Eur Heart J Cardiovasc Imaging* 2020;**21**:727–34.
  53. Kong WKF, Vollema EM, Prevedello F, Perry R, Ng ACT, Poh KK et al. Prognostic implications of left ventricular global longitudinal strain in patients with bicuspid aortic valve disease and preserved left ventricular ejection fraction. *Eur Heart J Cardiovasc Imaging* 2020;**21**:759–67.
  54. Ilardi F, Marchetta S, Martinez C, Sprynger M, Ancion A, Manganaro R et al. Impact of aortic stenosis on layer-specific longitudinal strain: relationship with symptoms and outcome. *Eur Heart J Cardiovasc Imaging* 2020;**21**:408–16.
  55. Vollema EM, Amanullah MR, Prihadi EA, Ng ACT, Van Der Bijl P, Sin YK et al. Incremental value of left ventricular global longitudinal strain in a newly proposed staging classification based on cardiac damage in patients with severe aortic stenosis. *Eur Heart J Cardiovasc Imaging* 2020;**21**:1248–58.
  56. Anand V, Adigun RO, Thaden JT, Pislaru SV, Pellikka PA, Nkomo VT et al. Predictive value of left ventricular diastolic chamber stiffness in patients with severe aortic stenosis undergoing aortic valve replacement. *Eur Heart J Cardiovasc Imaging* 2020;**21**:1160–8.
  57. Kellermair J, Saeed S, Ott HW, Kammler J, Blessberger H, Suppan M et al. High-molecular-weight von Willebrand Factor multimer ratio differentiates true-severe from pseudo-severe classical low-flow, low-gradient aortic stenosis. *Eur Heart J Cardiovasc Imaging* 2020;**21**:1123–30.
  58. Altes A, Ringle A, Bohbot Y, Bouchot O, Appert L, Guerbaai RA et al. Clinical significance of energy loss index in patients with low-gradient severe aortic stenosis and preserved ejection fraction. *Eur Heart J Cardiovasc Imaging* 2020;**21**:608–15.
  59. Holy EW, Nguyen-Kim TDL, Hoffelner L, Stocker D, Stadler T, Stähli BE et al. Multimodality imaging derived energy loss index and outcome after transcatheter aortic valve replacement. *Eur Heart J Cardiovasc Imaging* 2020;**21**:1092–102.
  60. Sønderskov PS, Lindholt JS, Hallas J, Gerke O, Hasifich S, Lambrechtsen J et al. Association of aortic valve calcification and vitamin K antagonist treatment. *Eur Heart J Cardiovasc Imaging* 2020;**21**:718–24.
  61. Postigo A, Pérez-David E, Revilla A, Raquel LA, González-Mansilla A, Prieto-Arévalo R et al. A comparison of the clinical efficacy of echocardiography and magnetic resonance for chronic aortic regurgitation. *Eur Heart J Cardiovasc Imaging* 2020;jeaa338.doi: 10.1093/ehjci/jeaa338.
  62. Vriesendorp MD, De Lind Van Wijngaarden RAF, Head SJ, Kappetein AP, Hickey GL, Rao V et al. The fallacy of indexed effective orifice area charts to predict prosthesis-patient mismatch after prosthesis implantation. *Eur Heart J Cardiovasc Imaging* 2020;**21**:1116–22.
  63. Winter M-P, Bartko PE, Krickl A, Gatterer C, Donà C, Nitsche C et al. Adaptive development of concomitant secondary mitral and tricuspid regurgitation after transcatheter aortic valve replacement. *Eur Heart J Cardiovasc Imaging* 2021;**22**:1045–53.
  64. Okuno T, Asami M, Khan F, Praz F, Heg D, Lanz J et al. Does isolated mitral annular calcification in the absence of mitral valve disease affect clinical outcomes after transcatheter aortic valve replacement? *Eur Heart J Cardiovasc Imaging* 2020;**21**:522–32.
  65. Stella S, Melillo F, Capogrosso C, Fiscaro A, Ancona F, Latib A et al. Intra-procedural monitoring protocol using routine transthoracic echocardiography with backup trans-oesophageal probe in transcatheter aortic valve replacement: a single centre experience. *Eur Heart J Cardiovasc Imaging* 2020;**21**:85–92.
  66. Koschutnik M, Dannenberg V, Nitsche C, Donà C, Siller-Matula JM, Winter M-P et al. Right ventricular function and outcome in patients undergoing transcatheter aortic valve replacement. *Eur Heart J Cardiovasc Imaging* 2021;**22**:1295–1303.
  67. Garg PK, Buzkova P, Meyghani Z, Budoff MJ, Lima J, Criqui M et al. Valvular calcification and risk of peripheral artery disease: the Multi-Ethnic Study of Atherosclerosis (MESA). *Eur Heart J Cardiovasc Imaging* 2020;**21**:1152–9.
  68. Chorin E, Rozenbaum Z, Topilsky Y, Konigstein M, Ziv-Baran T, Richert E et al. Tricuspid regurgitation and long-term clinical outcomes. *Eur Heart J Cardiovasc Imaging* 2020;**21**:157–65.
  69. Peri Y, Sadeh B, Sherez C, Hochstadt A, Biner S, Aviram G et al. Quantitative assessment of effective regurgitant orifice: impact on risk stratification, and cut-off for severe and torrential tricuspid regurgitation grade. *Eur Heart J Cardiovasc Imaging* 2020;**21**:768–76.
  70. Ortiz-Leon XA, Posada-Martinez EL, Trejo-Paredes MC, Ivey-Miranda JB, Pereira J, Crandall I et al. Understanding tricuspid valve remodelling in atrial fibrillation using three-dimensional echocardiography. *Eur Heart J Cardiovasc Imaging* 2020;**21**:747–55.
  71. Utsunomiya H, Harada Y, Susawa H, Ueda Y, Izumi K, Itakura K et al. Tricuspid valve geometry and right heart remodelling: insights into the mechanism of atrial functional tricuspid regurgitation. *Eur Heart J Cardiovasc Imaging* 2020;**21**:1068–78.
  72. Galea N, Catapano F, Marchitelli L, Cundari G, Maestrini V, Panebianco V et al. How to perform a cardio-thoracic magnetic resonance imaging in COVID-19: comprehensive assessment of heart, pulmonary arteries, and lung parenchyma. *Eur Heart J Cardiovasc Imaging* 2021;**22**:728–31.

73. Larsen CK, Aalen JM, Stokke C, Fjeld JG, Kongsgaard E, Duchenne J et al. Regional myocardial work by cardiac magnetic resonance and non-invasive left ventricular pressure: a feasibility study in left bundle branch block. *Eur Heart J Cardiovasc Imaging* 2020;**21**:143–53.
74. Bhuva AN, D'Silva A, Torlasco C, Nadarajan N, Jones S, Boubertakh R et al. Non-invasive assessment of ventriculo-arterial coupling using aortic wave intensity analysis combining central blood pressure and phase-contrast cardiovascular magnetic resonance. *Eur Heart J Cardiovasc Imaging* 2020;**21**:805–13.